APPLIED AND ENVIRONMENTAL MICROBIOLOGY, Oct. 2006, p. 6467–6473 Vol. 72, No. 10
0099-2240/06/$08.00+0 doi:10.1128/AEM.00417-06

Manganese(IV) Oxide Production by *Acremonium* sp. Strain KR21-2 and Extracellular Mn(II) Oxidase Activity

Naoyuki Miyata,[1]* Yukinori Tani,[1] Kanako Maruo,[2] Hiroshi Tsuno,[3]† Masahiro Sakata,[1] and Keisuke Iwahori[1]

Institute for Environmental Sciences[1] and Graduate School of Nutritional and Environmental Sciences,[2] University of Shizuoka, Shizuoka 422-8526, Japan, and National Institute of Advanced Industrial Science and Technology, Tsukuba 305-8569, Japan[3]

Received 20 February 2006/Accepted 19 July 2006

Ascomycetes that can deposit Mn(III, IV) oxides are widespread in aquatic and soil environments, yet the mechanism(s) involved in Mn oxide deposition remains unclear. A Mn(II)-oxidizing ascomycete, *Acremonium* sp. strain KR21-2, produced a Mn oxide phase with filamentous nanostructures. X-ray absorption near-edge structure (XANES) spectroscopy showed that the Mn phase was primarily Mn(IV). We purified to homogeneity a laccase-like enzyme with Mn(II) oxidase activity from cultures of strain KR21-2. The purified enzyme oxidized Mn(II) to yield suspended Mn particles; XANES spectra indicated that Mn(II) had been converted to Mn(IV). The pH optimum for Mn(II) oxidation was 7.0, and the apparent half-saturation constant was 0.20 mM. The enzyme oxidized ABTS [2,2′-azinobis(3-ethylbenzothiazoline-6-sulfonic acid)] (pH optimum, 5.5; K_m, 1.2 mM) and contained two copper atoms per molecule. Moreover, the N-terminal amino acid sequence (residues 3 to 25) was 61% identical with the corresponding sequence of an *Acremonium* polyphenol oxidase and 57% identical with that of a *Myrothecium* bilirubin oxidase. These results provide the first evidence that a fungal multicopper oxidase can convert Mn(II) to Mn(IV) oxide. The present study reinforces the notion of the contribution of multicopper oxidase to microbially mediated precipitation of Mn oxides and suggests that *Acremonium* sp. strain KR21-2 is a good model for understanding the oxidation of Mn in diverse ascomycetes.

Various microorganisms, including bacteria and fungi, transform Mn(II) to insoluble Mn(III, IV) oxides (7, 12, 36), and such microbial activity is believed to contribute to the occurrence of Mn oxides in aquatic and soil environments. These Mn oxides include fine-grained, poorly crystalline minerals such as vernadite, birnessite (layer type), and todorokite (tunnel type) (27). Vernadite (δ-MnO_2) is probably a class of birnessite that is disordered in the layer stacking direction or is composed of extremely thin plates (27, 41). Bacteriogenic Mn oxides closely resemble δ-MnO_2 or birnessite (35). Naturally occurring Mn oxide minerals extensively adsorb metal cations (e.g., Co, Ni, Zn, Cu, Mn, Pb, and Cd) and oxidize inorganic compounds [e.g., As(III) to As(V) and Cr(III) to Cr(IV)] and organic compounds (such as humic acids), making microbial Mn(II) oxidation significant in a biogeochemical context (35). Microbial Mn(II) oxidation also has potential environmental applications, including the removal of Mn and other trace metals from contaminated water (16, 23, 24, 34).

Many anamorphic fungi, including strains of *Acremonium*, *Coniothyrium*, *Cladosporium*, *Penicillium*, *Phoma*, and *Verticillium*, oxidize Mn(II) and deposit Mn oxides (6, 30, 32, 40). However, little is known about how these fungi oxidize Mn(II). Although Mn(II)-oxidizing fungi are widespread in aquatic and soil environments, their role in environmental Mn cycling has not been well understood. A recent study (37) found that several filamentous fungi can deposit Mn(IV) oxides in soil and proposed that these fungi contribute significantly to Mn oxidation in the soil.

White rot basidiomycetes excrete numerous Mn peroxidases (EC 1.11.1.13) that degrade lignin. These enzymes catalyze the oxidation of Mn(II) to Mn(III) by H_2O_2 in the presence of suitable Mn chelators, e.g., organic acids and pyrophosphate. Depletion of the chelator results in Mn(III) disproportionation to the solid form Mn(IV)O_2 (14, 26). Mn peroxidase purified from *Phanerochaete chrysosporium* produces insoluble Mn oxide in the absence of a chelator if H_2O_2 is supplied slowly by diffusion through a dialysis membrane (14). White rot basidiomycetes also excrete laccases (EC 1.10.3.2), a class of multicopper oxidases that catalyze one-electron oxidation of phenolic compounds by O_2. Typical laccases contain four Cu atoms (type 1, type 2, and two type 3 Cu atoms) and are blue due to absorption associated with the type 1 site at ~600 nm (31). Laccases from *Trametes versicolor* (17) and *Stropharia rugosoannulata* (28) can oxidize Mn(II) in the presence of a Mn chelator, leading to accumulation of soluble Mn(III)-chelate.

Although several enzymes may be responsible for Mn deposition by fungi, laccases are of particular interest due to their production by many basidiomycetes and ascomycetes (39) and because of the involvement of multicopper oxidase in the bacterial Mn(II) oxidation system(s) (5, 35, 36). However, the role of fungal laccases in Mn oxide formation has not been substantiated. Our working hypothesis is that enzymes with laccase-like activity, e.g., the enzyme produced by *Acremonium* sp. strain KR21-2 (22), could have an important role in Mn oxide formation. Our objective in this study was to purify this enzyme to homogeneity and characterize its properties. En-

* Corresponding author. Mailing address: Institute for Environmental Sciences, University of Shizuoka, 52-1 Yada, Suruga, Shizuoka 422-8526, Japan. Phone: 8154-264-5649. Fax: 8154-264-5594. E-mail: miyatan@smail.u-shizuoka-ken.ac.jp.

† Present address: Faculty of Education and Human Sciences, Yokohama National University, 79-2 Tokiwadai, Hodogaya, Yokohama 240-8501, Japan.

zymes with similar activity may occur in diverse ascomycete fungi.

MATERIALS AND METHODS

Organism. Strain KR21-2 has morphological traits typical of *Acremonium* spp. (22), and its 18S rRNA gene sequence (22) is most closely related to that of an *Acremonium* strain (42) (99% identical over 1,692 bp).

Enzyme purification. For enzyme purification, 50 ml of HEPES-buffered AY (HAY) medium supplemented with 1.0 μM $CuSO_4$ was inoculated with a conidial suspension of strain KR21-2 and cultured at 25°C (22). HAY medium contained 0.41 g of sodium acetate trihydrate, 0.15 g of yeast extract, 50 mg of $MgSO_4 \cdot 7H_2O$, 5.0 mg of K_2HPO_4, and 2.0 ml of trace mineral salts solution (22) per liter of 20 mM HEPES buffer (pH 7.0). At culture times of 50 to 54 h, when fungal growth had reached stationary phase, the entire culture was passed through a 25-μm mesh stainless-steel sieve and centrifuged (3,000 × *g*, 15 min, 10°C) to remove hyphae and conidia. The fungal growth in cultures was monitored by measuring the content of solid-state organic carbon with a Shimadzu TOC-5000A/SSM-5000A system (Shimadzu, Kyoto, Japan), as described previously (22). The supernatant fluid was concentrated ~100-fold by ultrafiltration (3,000 × *g*, 10°C) with a polyethersulfone membrane (molecular mass cutoff, 30 kDa; Vivascience, Lincoln, United Kingdom) and stored at −80°C. Samples concentrated from 3 liters of culture were combined, and ammonium sulfate was added to a final concentration of 0.6 M. This solution (30 ml) was loaded on a hydrophobic gel column (1 by 13 cm) packed with octyl-Sepharose CL-4B (Amersham Biosciences, Piscataway, NJ) that had been equilibrated with 20 mM HEPES (pH 7.0) containing 0.6 M ammonium sulfate. The column was washed with 60 ml of the HEPES at a flow rate of 22 ml h^{-1}, and adsorbed proteins were eluted with a linear gradient of ammonium sulfate (0.6 to 0 M) in HEPES and were monitored by absorbance at 280 nm (A_{280}). Fractions with 2,2′-azinobis(3-ethylbenzothiazoline-6-sulfonic acid) (ABTS)-oxidizing activity were combined, concentrated to 1 ml by ultrafiltration (3,000 × *g*, 10°C) using the polyethersulfone membrane, and then dialyzed three times against 500 ml of 5 mM HEPES (pH 7.0) at 4°C. The dialyzed sample was subdivided and applied to an anion-exchange Mono Q 5/50 GL column (Amersham Biosciences) equilibrated with 20 mM Tris-HCl (pH 7.6). Proteins were eluted at a flow rate of 1.0 ml min^{-1} with a timed program of linear gradients of NaCl (0 to 10 min, 0 to 0.2 M; 10 to 35 min, 0.2 to 0.5 M; and 35 to 40 min, 0.5 to 1.0 M). Active fractions were concentrated by ultrafiltration and dialyzed against 20 mM HEPES (pH 7.0) in a manner similar to that described above, and then frozen at −80°C.

Enzyme assays. Laccase activity was monitored by ABTS oxidation (4). The assay was routinely conducted in 20 mM HEPES buffer (pH 7.0) containing 0.5 mM ABTS at 30°C because in the previous study (22), ABTS-oxidizing activity of the spent culture medium could be detected under these conditions. The total volume of the reaction mixture was 1.0 ml. ABTS oxidation was measured by A_{420} (ε_{420} = 36 mM^{-1} cm^{-1}) (4). In some experiments, 0.5 mM 2,6-dimethoxyphenol was substituted for ABTS and its oxidation was monitored by A_{468} (ε_{468} = 30.5 mM^{-1} cm^{-1}) (17).

Mn(II) oxidase activity was determined with leucoberbelin blue, as described previously (21). The reaction was initiated by adding 20 μl of 5 mM $MnSO_4$ to a mixture containing 20 μl of enzyme sample and 60 μl of 20 mM HEPES (pH 7.0) at 30°C.

The effects of pH on enzymatic ABTS and Mn(II) oxidation were examined with 20 mM 2-morpholinoethanesulfonic acid (MES) at pH 4.5 to 7.0 and 20 mM HEPES buffers at pH 6.8 to 8.1. To examine enzyme kinetics, initial substrate concentrations were 0.1 to 4.0 mM for ABTS and 0.025 to 0.6 mM for Mn(II). The initial oxidation rates were applied to the Michaelis-Menten equation or the Hill equation, $v = V_{max} \times (S)^n/([S]^n + K_{0.5}{}^n)$. In the Hill equation, when $n = 1$, the equation is the same as the Michaelis-Menten equation, but K_m becomes $K_{0.5}$ (half-saturation constant). Nonlinear regression analysis was carried out with the Prism 3.0 software package (GraphPad Software, San Diego, CA). Protein concentration was determined with a bicinchoninic acid protein assay kit (Pierce, Rockford, IL).

The ABTS- and Mn(II)-oxidizing activities also were assayed in a 10% (wt/vol) polyacrylamide gel, as described previously (11), with modifications. After native polyacrylamide gel electrophoresis (PAGE) of the proteins, the gel was washed three times in 10 mM MES (pH 5.5) and incubated at 30°C in the same buffer containing 0.5 mM ABTS until a green color developed in the active regions. For Mn(II) oxidation, the gel was washed in 10 mM HEPES (pH 7.0) and incubated with 1 mM Mn(II). Proteins were identified by silver staining (25) with an assay kit from Wako Pure Chemical Industries (Osaka, Japan).

Mn oxide production. For production of Mn oxide in liquid culture, the fungus was grown in HAY with 1 mM $MnSO_4$ at 25°C for 7 days. Dissolved Mn(II) remaining in the supernatants was determined by inductively coupled plasma-mass spectrometry (ICP-MS) with a Hewlett-Packard model HP 4500 (Palo Alto, CA). Mn(II) decreased to <2 μM during cultivation. Mycelia with Mn-containing particles were rinsed in deionized water and suspended in 0.1 M sodium cacodylate (pH 7.4) containing 2% (vol/vol) glutaraldehyde for electron microscopy. For X-ray absorption near-edge structure (XANES) analysis, the washed samples were resuspended in deionized water and stored at −30°C.

The enzyme reaction was conducted in a mixture (800 μl) containing 1.5 μg of purified protein in 20 mM HEPES (pH 7.0) plus 1 mM $MnSO_4$ at room temperature. For electron microscopy, suspended Mn solids in the reaction mixture after 30 min of incubation were collected by centrifugation (15,000 × *g*, 10 min, 10°C), washed with deionized water, and air dried. In separate experiments the enzyme reaction was stopped at 10, 15, or 30 min by the addition of 10 mM sodium azide, and the mixtures were analyzed by XANES within 1 h of stopping the reaction.

Electron microscopy. For transmission electron microscopy (TEM), culture deposits were fixed with 2% (vol/vol) glutaraldehyde in 0.1 M sodium cacodylate (pH 7.4) overnight at 4°C, followed by fixation with 2% (wt/vol) OsO_4 in 0.1 M sodium cacodylate (pH 7.4) for 2 h at 4°C. Samples were dehydrated with an ethanol series (50% [vol/vol], 70%, 90%, 100%, and 100%; 20 min for each), followed by embedding in Epon 812 epoxy resin (Wako Pure Chemical Industries) for 48 h at 60°C. Ultrathin sections 80 to 90 nm thick were prepared using a diamond knife and an LKB Ultramicrotome 8800 (LKB, Stockholm, Sweden). Sections were poststained with 4% (wt/vol) uranyl acetate and 3% (wt/vol) lead citrate for 15 and 5 min, respectively, at room temperature. TEM was conducted with a JEOL JEM-2000EX (JEOL, Tokyo, Japan) at 100 kV.

For TEM of Mn oxide, the fixation and poststaining steps used for the culture deposits were omitted. An air-dried sample was embedded in epoxy resin, and ultrathin sections were prepared. A portion of the dried sample was observed directly with a JEOL JSM-6320F scanning electron microscope (SEM) (operated at 5 kV). TEM and SEM experiments were conducted at the Hanaichi Ultra-Structure Research Institute (Okazaki, Japan).

XANES spectroscopy. Mn K-edge XANES spectra were collected in fluorescence mode at beamline BL-12C of the Photon Factory of the High Energy Accelerator Research Organization (KEK-PF, Tsukuba, Japan), as described previously (21). Mn_2O_3 (99.9% pure; Kojundo Chemical Laboratories, Saitama, Japan) and vernadite (δ-MnO_2) (synthesized as described by Villalobos et al. [41]) were used as models for biogenic oxides. XANES spectra and average Mn oxidation numbers for these oxides have been published elsewhere (21). XANES spectra of the biogenic Mn oxide samples were normalized and fitted with a linear combination of normalized spectra of Mn(II) and δ-MnO_2 or a combination of Mn(II), δ-MnO_2, and Mn_2O_3. Calculations were made by the least-squares method using the REX2000 software package (Rigaku, Tokyo).

Enzyme analyses. The molecular mass of the denatured enzyme was estimated by conventional sodium dodecyl sulfate (SDS)-PAGE (19) with a set of markers, i.e., phosphorylase *b* (97.4 kDa), bovine serum albumin (66.3 kDa), aldolase (42.4 kDa), carbonic anhydrase (30.0 kDa), trypsin inhibitor (20.1 kDa), and lysozyme (14.4 kDa) (Daiichi Pure Chemicals, Tokyo), as molecular mass standards. The sample was mixed with 3× denaturant buffer (6% [wt/vol] SDS, 150 mM dithiothreitol, 0.01% [wt/vol] bromophenol blue, and 30% [wt/vol] glycerol in 0.2 M Tris-HCl [pH 6.8]) and either boiled for 2 min or left at room temperature for 24 h. The molecular mass of the native enzyme was estimated by gel filtration on a Superdex 75 10/300 GL column (Amersham Biosciences). Protein elution was conducted with 20 mM HEPES (pH 7.0) containing 0.15 M NaCl. Molecular mass markers consisted of bovine serum albumin (67.0 kDa), ovalbumin (43.0 kDa), chymotrypsinogen A (25.0 kDa), and RNase A (13.7 kDa) (Amersham Biosciences).

Metal contents were determined by liquid chromatography (LC)–ICP-MS. For LC, a Superdex 75 10/300 GL column was used, and the protein was eluted with 0.1 M ammonium acetate (pH 5.2) at a flow rate of 1.0 ml min^{-1} and monitored by A_{280}. The eluate was fed continuously to the inlet of the ICP-MS instrument to determine metal content, including Cu, Co, Mn, Ni, and Zn.

For N-terminal amino acid sequencing, denatured enzyme was run in an SDS-polyacrylamide gel and electroblotted onto a Sequi-Blot polyvinylidene difluoride membrane (Bio-Rad Laboratories, Hercules, CA). The protein band at 61 kDa visualized by Coomassie brilliant blue staining was excised and applied to a Hewlett-Packard HP G1005A system.

RESULTS

Mn(II) oxidation products produced by strain KR21-2. Mn(II) added at 1 mM to liquid cultures of *Acremonium* sp.

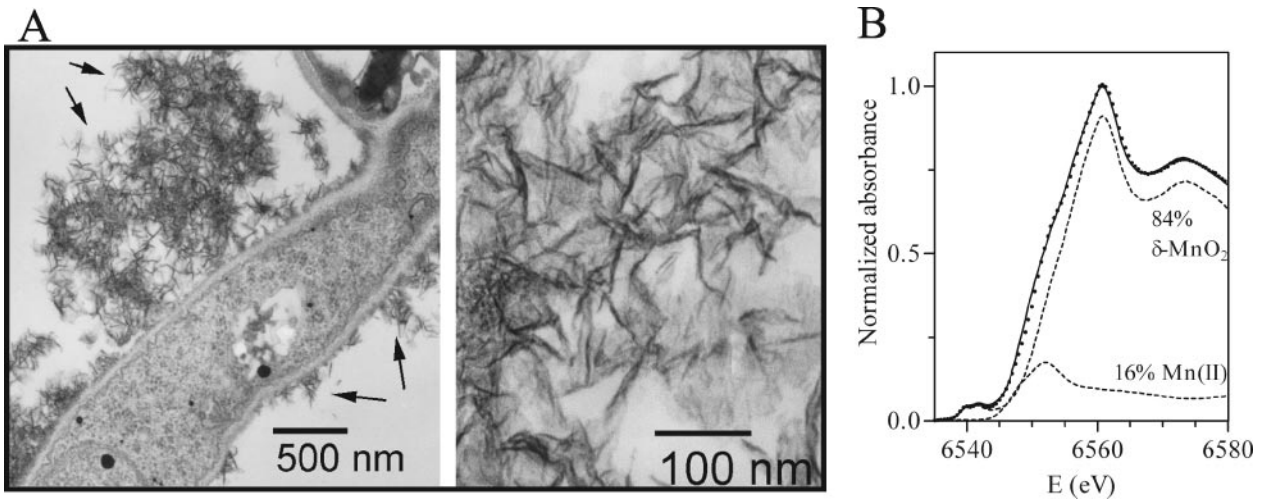

FIG. 1. TEM images (A) and Mn K-edge XANES spectrum (B) obtained from Mn deposits produced by *Acremonium* sp. strain KR21-2. (A) Arrows indicate electron-dense deposits, and the filamentous structures are enlarged in the right panel. (B) The spectrum (solid line) was fitted with a linear combination of normalized spectra of Mn(II) and δ-MnO_2. These fit components are presented as dashed lines, along with percent contributions. Dots represent the fitting result.

strain KR21-2 was oxidized beginning at 42 h and was almost completely precipitated (>99.8%) within 72 h. As before (22), fine Mn oxide particles (~2 μm in diameter) were observed on the mycelial surface. These particles had densely aggregated, filamentous structures (Fig. 1A). Some portions of the deposits were directly associated with the cell wall, but other portions were situated beyond the cell surface. These observations suggested that Mn(II) oxidation activity is located in the cell wall and also is excreted into the surrounding culture medium.

As Mn deposits of strain KR21-2 have an X-ray diffraction pattern of δ-MnO_2 with d-spacings of 2.4 Å and 1.4 Å (34), we used δ-MnO_2 as a model Mn(IV) oxide. The Mn K-edge XANES spectrum of the culture deposits had a maximum absorption peak at 6,561 eV (Fig. 1B), which is consistent with a solid Mn phase composed primarily of Mn(IV). Compared with the spectrum of δ-MnO_2, there was a slight shoulder at ~6,550 eV. The spectrum was well fitted with a linear combination of normalized spectra of δ-MnO_2 and Mn(II) (Fig. 1B), whose fractional contributions were estimated to be 84% and 16%, respectively. These observations confirmed the cooccurrence of Mn(II).

Purification of Mn(II)-oxidizing enzyme from strain KR21-2. When the concentrated supernatant was fractionated by octyl-Sepharose chromatography, ABTS-oxidizing activity was eluted

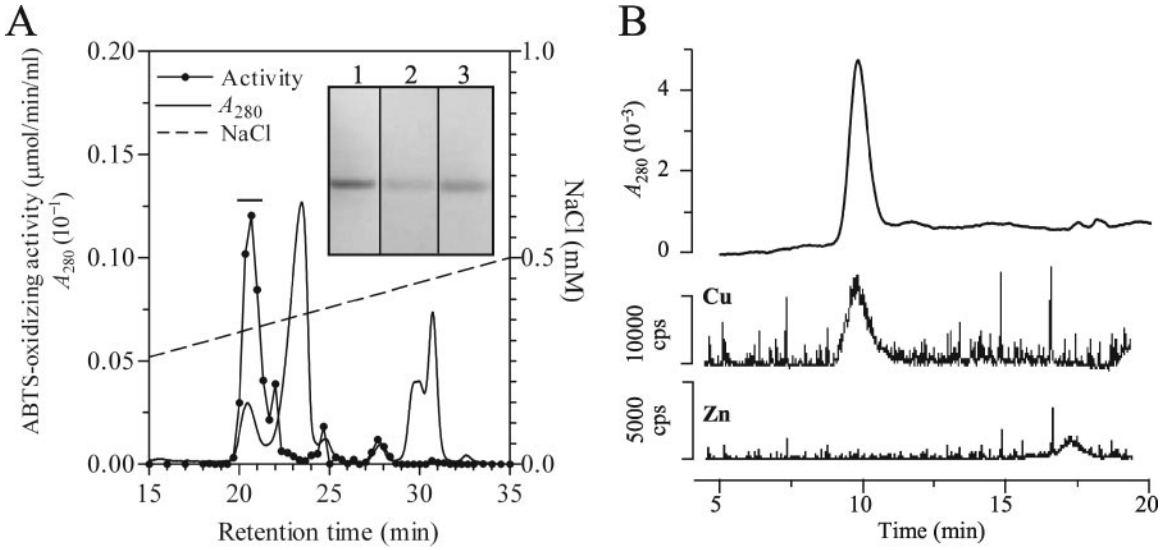

FIG. 2. (A) Purification of a laccase-like enzyme with Mn(II) oxidase activity from strain KR21-2 by Mono Q chromatography and native PAGE analysis of the purified enzyme (inset). The bar indicates the active fractions collected and used for further experiments. Inset, gel was stained with silver (lane 1) or was stained for Mn(II) (lane 2) and ABTS (lane 3) oxidation activity. The amount of protein loaded was 0.1 μg for each lane. The three visible bands exhibited equivalent migration. (B) LC–ICP-MS profile of the purified enzyme. Elution of the enzyme from a Superdex 75 column was monitored by A_{280}, and the eluate was continuously subjected to ICP-MS (chromatograms for Cu and Zn are shown).

TABLE 1. Purification of a laccase-like enzyme with Mn(II) oxidase activity from *Acremonium* sp. strain KR21-2

Purification step	Vol (ml)	Total amt of protein (mg)	Total activity[a] (U)	Sp act (U/mg)	Yield (%)	Purification (fold)
Crude concentrate[b]	30	1.8	3.5	1.9	100	1.0
Octyl-Sepharose	1.4	0.11	0.68	6.2	19	3.3
Mono Q	0.4	4.6×10^{-3}	0.14	30	4.0	16

[a] Activity was determined with ABTS (pH 7.0); one unit represents the amount of enzyme that oxidizes 1 μmol of ABTS per min.
[b] Concentrate was obtained from 3 liters of culture.

as a broad peak with decreasing ammonium sulfate concentration (from 0.3 to 0 M). The combined active fractions were applied to a Mono Q column (Fig. 2A), and four peaks with ABTS-oxidizing activity were resolved. The first major peak contained a single protein, as indicated by the results of native PAGE (Fig. 2A, inset) and gel filtration (Fig. 2B) (for the metal content, see below). The purified enzyme had Mn(II) oxidase activity. The specific ABTS-oxidizing activity increased 16-fold through the purification process (Table 1). Three minor peaks of activity (Fig. 2A) also contained proteins that could oxidize both ABTS and Mn(II) and that differed slightly in their electrophoretic migration when analyzed by native PAGE (data not shown). Thus, strain KR21-2 might produce several isozymes capable of oxidizing Mn(II). These minor peaks were not analyzed further.

The major band on SDS-PAGE has a molecular mass of 61 kDa, and there is a minor band with a molecular mass of ~45 kDa (data not shown). If the enzyme was loaded immediately after mixing with denaturants, then the opposite band pattern was obtained; i.e., the apparent 45-kDa band appeared to contain most of the protein. If the enzyme mixture was left at room temperature for several hours, the intensity of the 45-kDa band gradually decreased. These results strongly suggest that the apparent 45-kDa band represents an incompletely denatured form rather than a second protein. Using a Superdex 75 column, the molecular mass of the native enzyme was estimated to be 54 kDa, which was slightly lower than that determined by SDS-PAGE (61 kDa). The gel filtration analysis of the native enzyme may have underestimated the molecular mass, as the incompletely denatured enzyme resolved on SDS-PAGE appeared to exist in a compact form yielding a 45-kDa band. Thus, we concluded that the enzyme was a monomer with molecular mass of 61 kDa.

Mn(II) oxidation products produced by the KR21-2 enzyme. The purified enzyme in the presence of Mn(II) yielded suspended Mn solids that were present as spherical particles (0.7 to 1 μm in diameter) with erose surfaces (Fig. 3). The XANES spectra of the reaction mixtures (Fig. 4) indicated conversion of Mn(II) to Mn(IV), as demonstrated by the gradual appearance of an absorption peak at ~6,561 eV. Curve-fitting analyses with normalized spectra for Mn(II) and δ-MnO_2 showed an increase in the fractional contribution of δ-MnO_2 from 9% to 54% at 30 min (Fig. 4A to C). In the spectrum measured after 30 min of incubation, the maximum absorption peak shifted slightly (1 eV) to a lower-energy region relative to that of the absorption peak of δ-MnO_2. The curve-fitting result could be improved by using a linear combination of Mn(II) (43%), δ-MnO_2 (48%), and Mn_2O_3 (9%) (Fig. 4D). This result suggested that a minor amount (~10% of the total Mn) of Mn_2O_3 or other Mn(III) species may occur in the reaction mixture.

Properties of the strain KR21-2 enzyme. The optimal pH for Mn(II) oxidation was 7.0, with activity decreasing sharply as pH increased or decreased from 7.0 and with no activity detected at pH 5.4 or 8.1. Mn(II) oxidation rates at pH 7.0 exhibited sigmoidal substrate saturation kinetics. The apparent half-saturation constant ($K_{0.5}$) and V_{max} were 0.20 mM and 3.5 μmol min^{-1} mg^{-1}, respectively, when estimated with the Hill equation (constant $n = 3.6$; $r^2 > 0.99$). The pH optimum for ABTS oxidation was 5.5, and the activity decreased sharply as the pH decreased from 5.5 to 4.5, at which only 6% of the optimal activity was measured. The rates at pH 5.5 followed the Michaelis-Menten equation, with a K_m of 1.2 mM and a V_{max} of 250 μmol min^{-1} mg^{-1} ($r^2 > 0.98$). No oxidation of 2,6-dimethoxyphenol was observed at pH 5.5 or 7.0.

Based on LC–ICP-MS data (Fig. 2) and the molecular mass determined by SDS-PAGE (61 kDa), the Cu content of the purified enzyme was 2.2 atoms per molecule. No Zn (Fig. 2), Co, Ni, or Mn was detected during enzyme elution from the

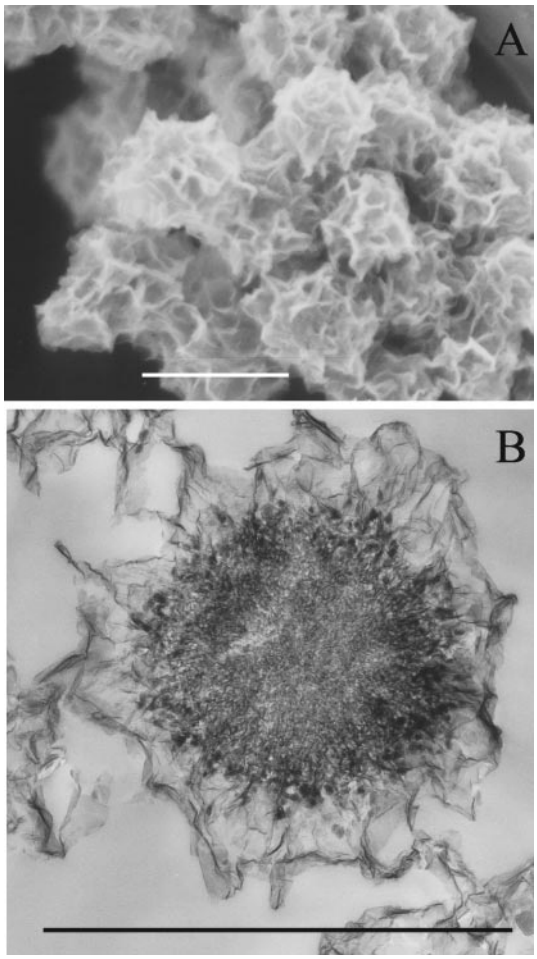

FIG. 3. SEM (A) and TEM images (B) of suspended Mn solids produced in the reaction mixture of Mn(II) and purified enzyme from *Acremonium* sp. strain KR21-2. Bars, 1 μm.

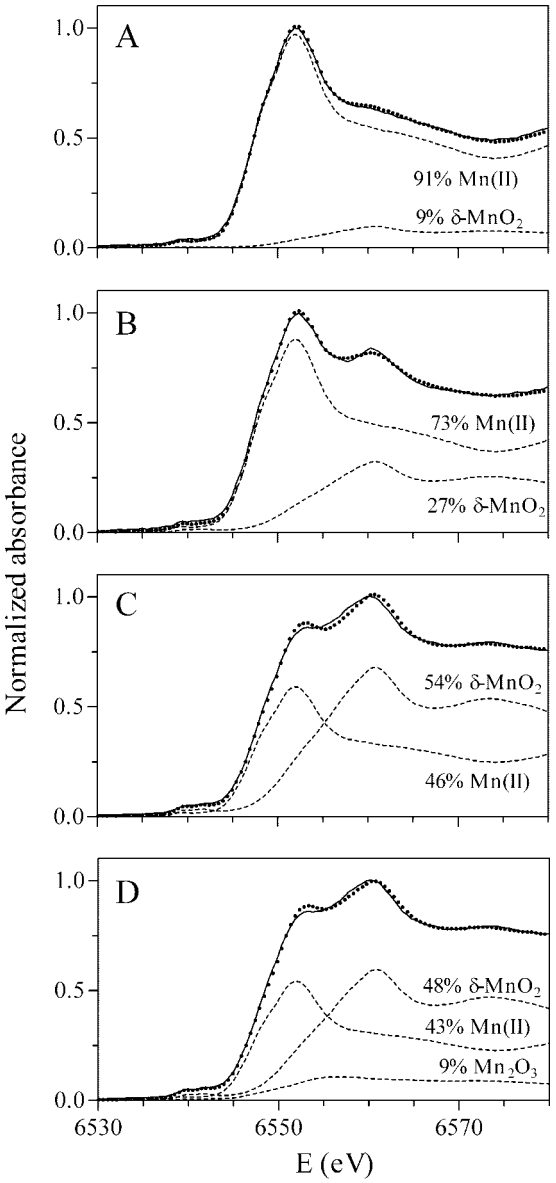

FIG. 4. Mn K-edge XANES spectra of reaction mixtures of Mn(II) and purified enzyme from *Acremonium* sp. strain KR21-2. Spectra (solid lines) measured after 10 (A), 15 (B), and 30 (C) min of incubation were fitted with a linear combination of normalized spectra of Mn(II) and δ-MnO_2. The spectrum in panel C was also fitted with a linear combination of Mn(II), Mn_2O_3, and δ-MnO_2 (D). Fit components are presented with dashed lines, along with percent contributions. Dots represent fitting results.

column. We did not have enough purified enzyme to reliably determine the UV-visible absorption spectrum.

The N-terminal amino acid sequence (25 residues) was XXDESPEYPLIYGKPLPIPPVKEPL (X, unidentified residue) and had significant homology with known multicopper oxidases, a polyphenol oxidase from *Acremonium murorum* (GenBank accession no. AJ271104) (15), and a bilirubin oxidase (EC 1.3.3.5) from *Myrothecium verrucaria* (D12579) (18). The amino acid sequence (residues 3 to 25) was 61% and 57% identical with the corresponding sequences of the *A. murorum* oxidase and the *M. verrucaria* oxidase, respectively.

DISCUSSION

The Mn oxide deposits produced by strain KR21-2 in culture are similar to those reported by Emerson et al. (9), who found that extracellular Mn(II)-oxidizing activity in an anamorphic fungus produced filamentous Mn oxide with a "*Metallogenium*" (8)-like structure. The observed nanostructural features could explain the relatively high Brunauer-Emmett-Teller surface area of the KR21-2 Mn oxide (113 $m^2\ g^{-1}$) (34). In addition, these features could at least partly explain the high sorption capacity of the KR21-2 oxide for metal cations [Zn(II), Mn(II), Co(II), and Ni(II)] (34) and the high reactivity with As(III) [oxidation to As(V)] (33).

We purified to homogeneity a Mn(II)-oxidizing enzyme from cultures of strain KR21-2. The fold purification was relatively low (16-fold), likely because the enzyme is produced in the culture as a major extracellular protein (22). The purified enzyme produced Mn oxide particles that had a fine-grained, densely packed interior, differing from previously described fungal and bacterial Mn oxides (9, 10, 12, 13). The formation of such relatively homogeneous particles may have resulted from the short-term (30-min), simple reaction system comprising only the enzyme, $MnSO_4$, and HEPES buffer. Similar morphotypes were not seen in the culture deposits (Fig. 1), which formed in the presence of complex cell components and exudates, and spent medium components, over a relatively long period [5 days after initiation of Mn(II) oxidation].

The enzymatically produced particles contained Mn(IV) oxide. Mn(IV) oxide minerals can form through disproportionation of Mn(III)-bearing oxides such as Mn_3O_4 and β-MnOOH, so that the primary product of the KR21-2 enzyme might be a Mn(III) oxide phase. However, this hypothesis is inconsistent with our results. The reaction conditions used [1 mM Mn(II); pH 7.0] are thermodynamically favorable for Mn(III) oxide precipitation, and under such conditions the disproportionation of Mn(III) oxides would proceed at a limited rate (20). Nevertheless, Mn(IV) oxide was produced quickly (within 10 min) in the reaction mixture, and Mn(III) species accounted for only ~10% of the total Mn (at 30 min), even if present. Thus, the results suggest that the primary product of the KR21-2 enzyme is a Mn(IV) oxide phase, not Mn(III) oxide.

The result of fitting for the 30-min incubation may rather represent the occurrence of Mn(III) species as a secondary product. Bargar et al. (2, 3) demonstrated that *Bacillus* spores precipitate a primary biotic product resembling δ-MnO_2 within several hours. The primal product reacts rapidly with Mn(II) to yield a secondary product, either layer-type MnO_2 or β-MnOOH, depending on the concentration of Mn(II) (likely below or above 0.5 mM, respectively) (2). Our result is consistent with this report. Under the reaction conditions used here, the remaining Mn(II) was still abundant [>40% of the initial Mn(II) (Fig. 4)]. It is likely, therefore, that the enzymatically occurring Mn(IV) oxide reacted with the remaining Mn(II) to form a thermodynamically stable Mn(III) phase. In contrast, Mn(III) species were not detected for the solid Mn phase produced in the fungal culture (Fig. 1). Dissolved Mn(II) de-

creased within 72 h to <2 μM, a concentration that is sufficiently low to minimize the formation of Mn(III) oxides (2, 20). Given the length of the culture period combined with the thermodynamic relations, Mn(III) oxide, even if it occurs abiotically, could be converted readily to a Mn(IV) oxide phase, as reported by Bargar et al. (2).

Based on the biochemical properties, we conclude that the Mn(II)-oxidizing enzyme of strain KR21-2 represents a class of multicopper oxidase. The molecular mass of the enzyme (61 kDa) is comparable to that of the multicopper oxidases of *M. verrucaria* (64 kDa) (18) and *A. murorum* (67 kDa; a protein expressed heterologously in *Aspergillus awamori*) (15). However, Mn(II) oxidation by these enzymes has not been reported. Although the KR21-2 enzyme appears to be a laccase, the catalytic properties for ABTS oxidation differ from those of common fungal laccases. The pH optimum, 5.5, is higher than those of other laccases (generally <4.0) (1), and its K_m, 1.2 mM, is approximately 1 to 2 orders of magnitude higher than those reported for other laccases (1). In addition, 2,6-dimethoxyphenol is a poor substrate for the KR21-2 enzyme. The *T. versicolor* laccase (17) that oxidizes Mn(II) to Mn(III) has low K_m values for ABTS (37 μM) and 2,6-dimethoxyphenol (15 μM) at pH 4.0, which are typical of common laccases (1). The kinetics for the organic substrates coupled with an N-terminal amino acid sequence closely related with that of a bilirubin oxidase (18) may indicate that the KR21-2 enzyme is not a true laccase. Multicopper oxidases contain at least four Cu atoms with a type 1 site and trinuclear clusters for substrate oxidation (31). Thus, our purified enzyme lacks two Cu atoms, although Thurston (39) argued that Cu atoms in laccases might be lost during the purification process.

Our study suggests that strain KR21-2 oxidizes Mn(II) in a manner similar to that used by bacteria such as *Bacillus* spp., *Leptothrix discophora*, and *Pseudomonas putida*, all of which possess multicopper oxidase-type Mn(II) oxidases (MnxG, MofA, and CumA, respectively) (5, 35, 36). The enzymatic Mn(II) oxidation by the *Bacillus* spores proceeds via two sequential one-electron transfers (43), i.e., Mn(II)→Mn(III)→Mn(IV), but the pathway in which the KR21-2 enzyme participates remains to be elucidated.

Our study provides the first evidence that a fungal multicopper oxidase can convert Mn(II) to Mn(IV) oxide and further emphasizes the importance of multicopper oxidase in microbially mediated precipitation of Mn oxides. Recently, we found that freshwater fungi, phylogenetically assigned to the orders *Xylariales* (one strain) and *Pleosporales* (three strains) of ascomycetes, deposit poorly crystalline oxides resembling δ-MnO_2 (21). As δ-MnO_2 is a class of birnessite (27, 41), our results are consistent with a report that the soil ascomycete *Gaeumannomyces graminis* produces a Mn(IV) oxide similar to birnessite (29). The four strains mentioned above (21) and *G. graminis* (38) also have laccase-like enzymes with Mn(II) oxidase activity. Therefore, phylogenetically diverse ascomycetes may use analogous enzymes to deposit Mn(IV) oxides. Our results suggest that *Acremonium* sp. strain KR21-2 is a good model for understanding the enzymatic oxidation of Mn by diverse ascomycetes and their role in the environment.

ACKNOWLEDGMENTS

The XANES experiments were performed with the approval of the Photon Factory Program Advisory Committee (2004G121).

This study was supported by the Institute for Environmental Sciences, University of Shizuoka, and by grants from the Ministry of Education, Culture, Sports, Science, and Technology of Japan (B16710052) and from the Japan Society for the Promotion of Science (C18510080).

We thank the reviewers for their comments and suggestions, which significantly improved the manuscript.

REFERENCES

1. **Baldrian, P.** 2006. Fungal laccases—occurrence and properties. FEMS Microbiol. Rev. **30:**215–242.
2. **Bargar, J. R., B. M. Tebo, U. Bergmann, S. M. Webb, P. Glatzel, V. Q. Chiu, and M. Villalobos.** 2005. Biotic and abiotic products of Mn(II) oxidation by spores of the marine *Bacillus* sp. strain SG-1. Am. Mineral. **90:**143–154.
3. **Bargar, J. R., B. M. Tebo, and J. E. Villinsky.** 2000. In situ characterization of Mn(II) oxidation by spores of the marine *Bacillus* sp. strain SG-1. Geochim. Cosmochim. Acta **64:**2775–2778.
4. **Bourbonnais, R., and M. G. Paice.** 1990. Oxidation of non-phenolic substrates. An expanded role for laccase in lignin biodegradation. FEBS Lett. **267:**99–102.
5. **Brouwers, G. J., E. Vijgenboom, P. L. A. M. Corstjens, J. P. M. de Vrind, and E. W. de Vrind-de Jong.** 2000. Bacterial Mn^{2+} oxidizing systems and multicopper oxidases: an overview of mechanisms and functions. Geomicrobiol. J. **17:**1–24.
6. **De la Torre, M. A., and G. Gomez-Alarcon.** 1994. Manganese and iron oxidation by fungi isolated from building stone. Microb. Ecol. **27:**177–188.
7. **Ehrlich, H. L.** 2002. Geomicrobiology, 4th ed., p. 429–528. Marcel Dekker, New York, N.Y.
8. **Emerson, D.** 2000. Microbial oxidation of Fe(II) and Mn(II) at circumneutral pH, p. 31–52. *In* D. R. Lovley (ed.), Environmental microbe-metal interaction. ASM Press, Washington, D.C.
9. **Emerson, D., R. E. Garen, and W. C. Ghiorse.** 1989. Formation of *Metallogenium*-like structures by a manganese-oxidizing fungus. Arch. Microbiol. **151:**223–231.
10. **Francis, C. A., K. L. Casciotti, and B. M. Tebo.** 2002. Localization of Mn(II)-oxidizing activity and the putative multicopper oxidase, MnxG, to the exosporium of the marine *Bacillus* sp. strain SG-1. Arch. Microbiol. **178:**450–465.
11. **Francis, C. A., E. M. Co, and B. M. Tebo.** 2001. Enzymatic manganese(II) oxidation by a marine α-proteobacterium. Appl. Environ. Microbiol. **67:** 4024–4029.
12. **Ghiorse, W. C.** 1984. Biology of iron- and manganese-depositing bacteria. Annu. Rev. Microbiol. **38:**515–550.
13. **Ghiorse, W. C., and P. Hirsch.** 1979. An ultrastructural study of iron and manganese deposition associated with extracellular polymers of *Pedomicrobium*-like budding bacteria. Arch. Microbiol. **123:**213–226.
14. **Glenn, J. K., L. Akileswaran, and M. H. Gold.** 1986. Mn(II) oxidation is the principal function of the extracellular Mn-peroxidase from *Phanerochaete chrysosporium*. Arch. Biochem. Biophys. **251:**688–696.
15. **Gouka, R. J., M. van der Heiden, T. Swarthoff, and C. T. Verrips.** 2001. Cloning of a phenol oxidase gene from *Acremonium murorum* and its expression in *Aspergillus awamori*. Appl. Environ. Microbiol. **67:**2610–2626.
16. **Hallberg, K. B., and D. B. Johnson.** 2005. Biological manganese removal from acid mine drainage in constructed wetlands and prototype bioreactors. Sci. Total Environ. **338:**115–124.
17. **Höfer, C., and D. Schlosser.** 1999. Novel enzymatic oxidation of Mn^{2+} to Mn^{3+} catalyzed by a fungal laccase. FEBS Lett. **451:**186–190.
18. **Koikeda, S., K. Ando, H. Kaji, T. Inoue, S. Murao, K. Takeuchi, and T. Samejima.** 1993. Molecular cloning of the gene for bilirubin oxidase from *Myrothecium verrucaria* and its expression in yeast. J. Biol. Chem. **268:**18801–18809.
19. **Laemmli, U. K.** 1970. Cleavage of structural proteins during the assembly of the head of bacteriophage T4. Nature **227:**680–685.
20. **Mandernack, K. W., J. Post, and B. M. Tebo.** 1995. Manganese mineral formation by bacterial spores of the marine *Bacillus*, strain SG-1: evidence for the direct oxidation of Mn(II) to Mn(VI). Geochim. Cosmochim. Acta **59:**4393–4408.
21. **Miyata, N., K. Maruo, Y. Tani, H. Tsuno, H. Seyama, M. Soma, and K. Iwahori.** 2006. Production of biogenic manganese oxides by anamorphic ascomycete fungi isolated from streambed pebbles. Geomicrobiol. J. **23:**63–73.
22. **Miyata, N., Y. Tani, K. Iwahori, and M. Soma.** 2004. Enzymatic formation of manganese oxides by an *Acremonium*-like hyphomycete fungus, strain KR21-2. FEMS Microbiol. Ecol. **47:**101–109.
23. **Nelson, Y. M., L. W. Lion, W. C. Ghiorse, and M. L. Shuler.** 1999. Production of biogenic Mn oxides by *Leptothrix discophora* SS-1 in a chemically defined growth medium and evaluation of their Pb adsorption characteristics. Appl. Environ. Microbiol. **65:**175–180.

24. **Nelson, Y. M., L. W. Lion, M. L. Shuler, and W. C. Ghiorse.** 2002. Effect of oxide formation mechanisms on lead adsorption by biogenic manganese (hydr)oxides, iron (hydr)oxides, and their mixtures. Environ. Sci. Technol. **36:**421–425.
25. **Oakley, B. R., D. R. Kirsch, and N. R. Morris.** 1980. A simplified ultrasensitive silver stain for detecting proteins in polyacrylamide gels. Anal. Biochem. **105:**361–363.
26. **Perez, J., and T. W. Jeffries.** 1992. Roles of manganese and organic acid chelators in regulating lignin degradation and biosynthesis of peroxidases by *Phanerochaete chrysosporium*. Appl. Environ. Microbiol. **58:**2402–2409.
27. **Post, J. E.** 1999. Manganese oxide minerals: crystal structures and economic and environmental significance. Proc. Natl. Acad. Sci. USA **96:**3447–3454.
28. **Schlosser, D., and C. Höfer.** 2002. Laccase-catalyzed oxidation of Mn^{2+} in the presence of natural Mn^{3+} chelators as a novel source of extracellular H_2O_2 production and its impact on manganese peroxidase. Appl. Environ. Microbiol. **68:**3514–3521.
29. **Schulze, D. G., T. McCay-Buis, S. R. Sutton, and D. M. Huber.** 1995. Manganese oxidation states in *Gaeumannomyces*-infested wheat rhizospheres probed by micro-XANES spectroscopy. Phytopathology **85:**990–994.
30. **Schweisfurth, R.** 1971. Manganoxidierende Pilze. I. Vorkommen, Isolierungen und mikroskopische Untersuchungen. Z. Allg. Mikrobiol. **11:**415–430.
31. **Solomon, E. I., U. M. Sundaram, and T. E. Machonkin.** 1996. Multicopper oxidases and oxygenases. Chem. Rev. **96:**2563–2605.
32. **Sterflinger, K.** 2000. Fungi as geologic agents. Geomicrobiol. J. **17:**97–124.
33. **Tani, Y., N. Miyata, M. Ohashi, T. Ohnuki, H. Seyama, K. Iwahori, and M. Soma.** 2004. Interaction of inorganic arsenic with biogenic manganese oxide produced by a Mn-oxidizing fungus, strain KR21-2. Environ. Sci. Technol. **38:**6618–6624.
34. **Tani, Y., M. Ohashi, N. Miyata, H. Seyama, K. Iwahori, and M. Soma.** 2004. Sorption of Co(II), Ni(II), and Zn(II) on biogenic manganese oxides produced by a Mn-oxidizing fungus, strain KR21-2. J. Environ. Sci. Health A **39:**2641–2660.
35. **Tebo, B. M., J. R. Bargar, B. G. Clement, G. J. Dick, K. J. Murray, D. Parker, R. Verity, and S. M. Webb.** 2004. Biogenic manganese oxides: properties and mechanisms of formation. Annu. Rev. Earth Planet. Sci. **32:**287–328.
36. **Tebo, B. M., H. A. Johnson, J. K. McCarthy, and A. S. Templeton.** 2005. Geomicrobiology of manganese(II) oxidation. Trends Microbiol. **13:**421–428.
37. **Thompson, I. A., D. M. Huber, C. A. Guest, and D. G. Schultze.** 2005. Fungal manganese oxidation in a reduced soil. Environ. Microbiol. **7:**1480–1487.
38. **Thompson, I. A., D. M. Huber, and D. G. Schultze.** 2006. Evidence of a multicopper oxidase in Mn oxidation by *Gaeumannomyces graminis var. tritici*. Phytopathology **96:**130–136.
39. **Thurston, C. F.** 1994. The structure and function of fungal laccases. Microbiology **140:**19–26.
40. **Timonin, M. I., W. I. Illman, and T. Hartgerink.** 1972. Oxidation of manganous salts of manganese by soil fungi. Can. J. Microbiol. **18:**793–799.
41. **Villalobos, M., B. Toner, J. Bargar, and G. Sposito.** 2003. Characterization of the manganese oxide produced by *Pseudomonas putida* strain MnB1. Geochim. Cosmochim. Acta **67:**2649–2662.
42. **Watanabe, K., N. Takihana, H. Aoyagi, S. Hanada, Y. Watanabe, N. Ohmura, H. Saiki, and H. Tanaka.** 2005. Symbiotic association in *Chlorella* culture. FEMS Microbiol. Ecol. **51:**187–196.
43. **Webb, S. M., G. J. Dick, J. R. Bargar, and B. M. Tebo.** 2005. Evidence for the presence of Mn(III) intermediates in the bacterial oxidation of Mn(II). Proc. Natl. Acad. Sci. USA **102:**5558–5563.